

---

# SpecNet: Spectral Domain Convolutional Neural Network

---

**Bochen Guan\*, Jinnian Zhang\*, and William A. Sethares**

Department of Electrical and Computer Engineering  
University of Wisconsin-Madison  
Madison, WI, 53705, USA  
{gbochen, jinnian.zhang, vjog, sethares}@wisc.edu

**Richard Kijowski and Fang Liu**

University of Wisconsin-Madison  
Department of Radiology  
Madison, WI, 53705, USA  
rkijowski@uwhealth.org, fliu37@wisc.edu

## Abstract

The memory consumption of most Convolutional Neural Network (CNN) architectures grows rapidly with increasing depth of the network, which is a major constraint for efficient network training and inference on modern GPUs with yet limited memory. Several studies show that the feature maps (as generated after the convolutional layers) are the big bottleneck in this memory problem. Often, these feature maps mimic natural photographs in the sense that their energy is concentrated in the spectral domain. This paper proposes a Spectral Domain Convolutional Neural Network (SpecNet) that performs both the convolution and the activation operations in the spectral domain to achieve memory reduction. SpecNet exploits a configurable threshold to force small values in the feature maps to zero, allowing the feature maps to be stored sparsely. Since convolution in the spatial domain is equivalent to a dot product in the spectral domain, the multiplications only need to be performed on the non-zero entries of the (sparse) spectral domain feature maps. SpecNet also employs a special activation function that preserves the sparsity of the feature maps while effectively encouraging the convergence of the network. The performance of SpecNet is evaluated on three competitive object recognition benchmark tasks (MNIST, CIFAR-10, and SVHN), and compared with four state-of-the-art implementations (LeNet, AlexNet, VGG, and DenseNet). Overall, SpecNet is able to reduce memory consumption by about 60% without significant loss of performance for all tested network architectures.

## 1 Introduction

Deep convolutional neural networks have made significant progress on various tasks in recent years [1–6]. Current successful deep CNNs such as ResNet [7] and DenseNet [8] typically include over 100 layers and require large amounts of training data. Training these models becomes computationally and memory intensive, especially when limited resources are available [9]. Therefore, it is essential to reduce the memory requirements to allow better network training and deployment, such as deploying deep CNNs on embedded systems and cell phones.

---

\*Authors contributed equally to this work

Several studies [10, 11] show that the intermediate layer outputs (feature maps) are the primary contributors to this memory bottleneck. Existing methods such as model compression [12–15] and scheduling [16–18], do not directly address the storage of feature maps. By transforming the convolutions into the spectral domain, we target the memory requirements of feature maps.

In contrast to [10], which proposes an efficient encoded representation of feature maps in the spatial domain, we exploit the property that the energy of feature maps is concentrated in the spectral domain [10]. Values that are less than a configurable threshold are forced to zero, so that the feature maps can be stored sparsely. We call this approach the Spectral Domain Convolutional Neural Network (SpecNet). In this new architecture, convolutional and activation layers are implemented in the spectral domain. The outputs of convolutional layers are equal to the multiplication of non-zero entries of the inputs and kernels. The activation function is designed to preserve the sparsity and symmetry properties of the feature maps in the spectral domain, and also allow effective derivative computation in backward propagation.

More specifically, this paper contributes the following:

- A new CNN architecture (SpecNet) that performs convolution and activation in the spectral domain. Feature maps are thresholded and compressed to allow reducing model memory by only computing and saving non-zero entries.
- A spectral domain activation function is applied to both the real and imaginary parts of the input feature maps, preserving the sparsity property and ensuring effective network convergence during training.
- Extensive experiments are conducted to show the effectiveness of SpecNet using different architectures at multiple computer vision tasks. For example, a SpecNet implementation of DenseNet architecture can reach up to 60% reduction of the memory consumption on the SHVN dataset without significant loss of accuracy (95.8% testing accuracy compared with 98.2% accuracy of the original implementation).

## 2 Related Work

### 2.1 Model Compression

Model compression can be achieved by using several approaches including quantization, pruning and weight decomposition.

In the approach of quantization, the values of filter kernels in the convolutional layers and weight matrices in fully-connected layers are quantized into limited levels which can decrease the computational complexity and reduce memory cost [12, 19]. The extreme case of quantization is binarization [13, 20] which uses only +1 and −1 to represent each value of the weight, resulting in dramatic memory reduction but raising risks for potentially degraded performance.

Pruning and weight decomposition are other approaches for model compression. The key idea in pruning is to remove unimportant connections. Some initial work [14] focused on using weight decay to sparsify the connections in neural networks while more recent work [21, 22] applied structured sparsity regularizers to the weights. Instead of selecting redundant connections, [23] proposed a compression technique that fixed a random connectivity pattern and required the CNN to train around it. Weight decomposition is based on a low-rank decomposition of the weights in the network. SVD is an efficient decomposition method, and has proven to be successful in shrinking the size of the model [15]. Other work [24, 25] uses PCA to make the rank selection. The pruning and weight decomposition attempt to reduce the size of the model so that it is more easily deployed in embedded systems or smart phones. Overall, the aforementioned methods are focused on compressing weights to reduce the model size, and further reduce the size of feature maps. SpecNet is an orthogonal method directly reduce the memory consumption by sparsify the feature maps and store it efficiently. Both methods can be mutually applied to save memory.

### 2.2 Memory Sharing

Since the life time of feature maps is different in each layer, it is possible to design data reuse pattern to reduce memory consumption. [16] observes the feature maps in some layers that are responsible

for most of the memory consumption are relatively cheap to compute. Then by storing the output of the concatenation, batch normalization and ReLU layers in shared memory, DenseNet can achieve more than 4x memory saving, compared to the original implementation that allocates new memory for these layers. A more general algorithm for designing memory sharing patterns can be found in [17]. It can be applied to CNNs and RNNs with sublinear memory cost than their original implementations. Recently, An approach called SmartPool [18] has been proposed to provide even more fine-grained memory sharing strategy to boost the memory reduction performance.

### 2.3 Representation of Feature Maps in the Spatial Domain

The above methods are not focused on compressing feature maps directly. [10] employed two classes of layer-specific encoding schemes to encode and store the feature maps in the time domain, and to decode the data for back propagation. The additional encoding and decoding process will increase the computational complexity. In SpecNet, the architecture is designed for sparse storage of feature maps in the spectral domain, which is more computationally efficient.

[11] proposed a method to extract intrinsic representation of the feature maps while preserving the discriminability of the features. It can achieve a high compression ratio, but the training process involves a pre-trained CNN and solving an optimization problem. SpecNet does not require additional modules in the training process and is easier to implement.

### 2.4 CNN in the Spectral Domain

A few pilot studies have attempted to combine Fast Fourier Transform (FFT) and Wavelet transform with CNNs [26–28]. However, most of these works aim to make the training process faster by replacing the traditional convolution operation with FFT and dot product of the inputs and kernel in spectral domain [26, 27]. Wavelet CNN [28] concatenates the feature maps and multi-resolution features captured by the wavelet transform of the input images to improve the classification accuracy. These methods do not attempt to reduce memory, and several works (such as the Wavelet CNN) require more memory in order to achieve optimal performance. In contrast, SpecNet uses the FFT to reduce memory consumption and its computation complexity depending on various input parameters, which is quite different from most FFT-based CNN implementations.

## 3 Spectral Domain Convolutional Neural Network

The key idea of SpecNet rests on the observation that feature maps, like most natural images, tend to have compact energy in the spectral domain. the compression can be achieved by only keeping non-trivial values while zeroing out small entries that hold trivial information. A threshold ( $\beta$ ) can then be applied to configure compression rate where larger  $\beta$  value results in more zeros in feature maps in spectral domain.

As with existing CNNs [29, 30, 8, 31] which operate in the spatial domain, the elemental SpecNet, operating in the spectral domain, also consists of three layers: convolutional layers, activation layers, and pooling layers as shown at the bottom half of Fig. 1. Notably, in contrast to previous study [26–28] that simply uses FFT for accelerating network training, SpecNet represents a complete new design of the network architecture for convolution, tensor compression, and activation in the spectral domain for both forward and backward propagation in network training and inference.

### 3.1 Convolution in the Spectral Domain

Consider 2D-convolution with a stride of 1. In a standard convolutional layer, the output is computed by

$$y(i, j) = x * k = \sum_{m=0}^{M-1} \sum_{n=0}^{N-1} x(m, n) \cdot k(i - m, j - n), \quad (1)$$

where  $x$  is an input matrix of size  $(M, N)$ ;  $k$  is the kernel with dimension  $(N_k, N_k)$ , and  $*$  indicates 2D convolution. The output  $y$  in the spatial domain has dimensions  $(M', N')$ , where  $M' = M + N_k - 1$  and  $N' = N + N_k - 1$ . This process involves  $\mathcal{O}(M'N'N_k^2)$  multiplications.

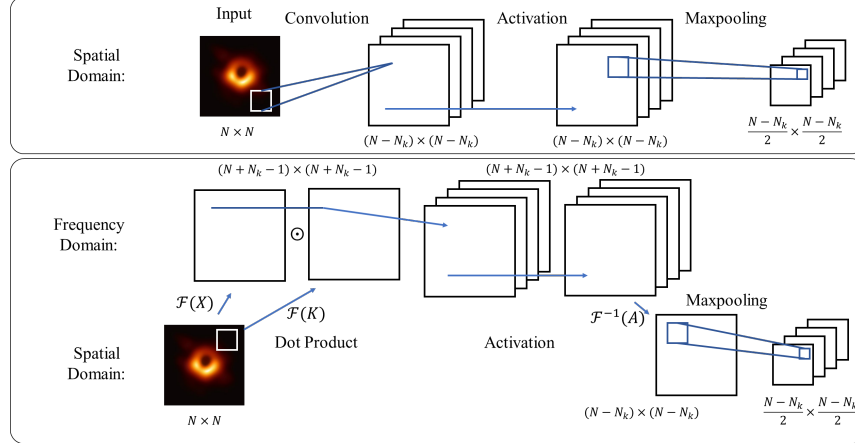


Figure 1: The standard convolutional block in spatial and spectral domain. The top figure shows the standard convolutional block containing an input layer, a convolutional layer followed by an activation layer and a maxpooling layer. The bottom figure shows the convolutional block in SpecNet. The kernels are stored in the spatial domain the feature maps are efficiently stored in spectral domain.

Convolution can be implemented more efficiently in the spectral domain as

$$Y = X \odot K, \quad (2)$$

where  $X$  is the transformed input in the spectral domain by FFT  $X = \mathcal{F}(x)$ , and  $K$  is the corresponding kernel in the spectral domain,  $K = \mathcal{F}(k)$ .  $\odot$  represents element-by-element multiplication, which requires equal dimensions for  $X$  and  $K$ . Therefore,  $x$  and  $k$  are zero-padded to match their dimensions  $(M', N')$ . Since there are various hardware optimizations for the FFT [32, 33, 26], it requires  $\mathcal{O}(M'N' \log(M'N'))$  complex multiplications. The computational complexity of (2) is  $\mathcal{O}(M'N')$  and so the overall complexity in the spectral domain is  $\mathcal{O}(M'N' \log(M'N'))$ . Depending on the size of the inputs and kernels, the SpecNet can have a computation advantage in contrast to spatial convolution in some cases [26, 27]. However, SpecNet is focused on reducing memory consumption for applications that are primarily limited by the available memory.

The compression of  $Y$  involves a configurable threshold  $\beta$ , which forcing small absolute values (lower than  $\beta$ ) of the entries in  $Y$  to zero. This compression let the thresholded map  $(\hat{Y})$  be sparse and we only store non-zero entries in  $\hat{Y}$  to save memory.

The backward propagation step requires the calculation of the error  $\delta_X$  for the previous layers, and the gradients  $\Delta_K$  for  $k$ . Let  $\delta_Y$  be the error from the next layer, and  $X_0, k_0$  be the input and kernel of the convolutional layer stored in the forward propagation, respectively. Then

$$\begin{aligned} \delta_X &= \nabla_X L|_{X=X_0} = \delta_Y \odot K_0 \\ \Delta_K &= \nabla_K L|_{K=\mathcal{F}(k_0)} = \delta_Y \odot X_0, \end{aligned} \quad (3)$$

where  $L$  is the loss function. After obtaining its gradient in the spectral domain  $\Delta_K$ , the IFFT is applied. Then the  $N_k \times N_k$  matrix for the update of  $k$  can be expressed as

$$k_1 = k_0 + \lambda[\mathcal{F}^{-1}(\Delta_K)]_{N_k \times N_k}, \quad (4)$$

where  $\lambda$  is the learning rate. The kernels are updated after obtaining  $\Delta_K$ , the gradient in the spectral domain, by using inverse FFT and downsampling.

Note that after the gradient update of  $\Delta_K$ , the kernel is further converted from spectral domain back into spatial domain using inverse FFT to save kernel storage.

A more general case of 2D-convolution with arbitrary integer stride can be viewed as a combination of 2D-convolution with stride of 1 and uniform down-sampling. This can also be implemented in the spectral domain [26].

---

**Algorithm 1** Forward propagation of the convolutional block in spectral domain

---

**Input:** feature maps  $x$  from the last layer with size of  $M \times N$ ; kernel  $k$  ( $N_k \times N_k$ ); threshold  $\beta$ .

```
1: if  $x$  in the spectral domain then
2:   Set  $M' = M$ ,  $N' = N$  and  $X = x$ .
3: else
4:   Set  $M' = M + N_k - 1$  and  $N' = N + N_k - 1$ .
5: end if
6: for  $i = 1$  to  $M'$  do
7:   for  $j = 1$  to  $N'$  do
8:     if  $X$  is None then
9:        $\hat{x}(i, j) = x(i, j)$  if  $i \leq M$  and  $j \leq N$ , and  $\hat{x}(i, j) = 0$  otherwise.
10:    end if
11:     $\hat{k}(i, j) = k(i, j)$  if  $i \leq N_k$  and  $j \leq N_k$ , and  $\hat{k}(i, j) = 0$  otherwise.
12:    Calculate  $K = \mathcal{F}(\hat{k})$  and  $X = \mathcal{F}(\hat{x})$  if  $X$  is None.
13:  end for
14: end for
15: Calculate  $Y$  after convolution according to (2).
16: Obtain  $\hat{Y}$  where  $\hat{Y}(i, j) = Y(i, j)$  if  $|Y(i, j)| > \beta$ , and  $\hat{Y}(i, j) = 0$  otherwise.
17: Get  $Z = f(\hat{Y})$  where  $f$  is defined in (5)
```

**Output:** The feature map in the spectral domain:  $Z$ .

---

### 3.2 Activation Function in the Spectral Domain

In SpecNet, the activation function for the feature maps is designed to perform directly in the spectral domain. For each complex entries in the spectral feature map, there is

$$f(a + ib) = h(a) + ig(b) \quad (5)$$

where

$$h(x) = g(x) = \tanh(x) = \frac{e^x - e^{-x}}{e^x + e^{-x}}. \quad (6)$$

We selected the tanh function in (5) function as a proof-of-concept design in this current study. Other activation formula might also be functional given several rules for  $h(x)$  and  $g(x)$  as follows:

1. They allow inexpensive gradient calculation.
2. Both  $g(x)$  and  $h(x)$  are monotonic nondecreasing
3. The functions are odd, i.e.  $g(-x) = -g(x)$ .

The first and second rules are standard requirements for nearly all popular activation functions used in modern CNN design. The third rule in SpecNet is applied to preserve the conjugate symmetry structure of the spectral feature maps so that they can be converted back into real spatial features without generating pseudo phases. By looking at the 2D FFT,

$$X(p, q) = \mathcal{F}(x) = \sum_{m=0}^{M+N_k-2} \sum_{n=0}^{N+N_k-2} w_M^{pm} w_N^{qn} x(m, n) \quad (7)$$

where  $w_M = e^{-2\pi i/(M+N_k-1)}$  and  $w_N = e^{-2\pi i/(N+N_k-1)}$ . If  $x$  is real, i.e. the conjugate of  $x$  is itself ( $\bar{x} = x$ ), then

$$\begin{aligned} X(M + N_k - 1 - p_0, N + N_k - 1 - q_0) \\ &= \sum_{m=0}^{M+N_k-2} \sum_{n=0}^{N+N_k-2} w_M^{(M+N_k-1-p_0)m} w_N^{(N+N_k-1-q_0)n} x(m, n) \\ &= \sum_{m=0}^{M+N_k-2} \sum_{n=0}^{N+N_k-2} w_M^{-p_0m} w_N^{-q_0n} x(m, n) \\ &= \overline{X(p_0, q_0)} \end{aligned} \quad (8)$$

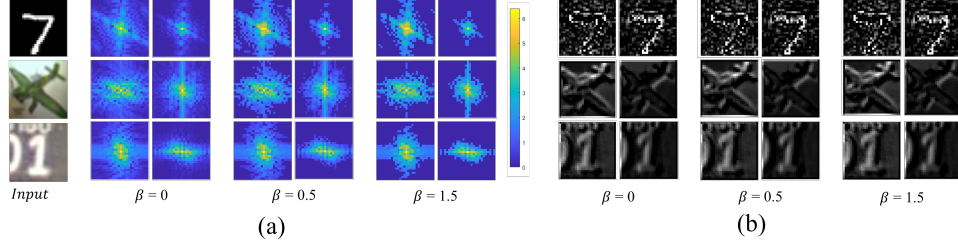


Figure 2: Feature maps of SpecDenseNet after first convolutional layer of different inputs. (a) Feature maps after two different kernels in spectrum domain under three different thresholds ( $\beta$ ). (b) Feature maps, converted from spectrum domain to spatial domain by utilizing inverse Fourier transform, under different thresholds ( $\beta$ )

Therefore,  $g(x)$  must be odd to retain the symmetry structure of the activation layer to ensure that

$$f(\overline{a + ib}) = h(a) + ig(-b) = h(a) - ig(b) = \overline{f(a + ib)}. \quad (9)$$

If the symmetry structure of  $\delta_Y$  in (3) is also maintained, the gradients in the spatial domain should be real after the inverse FFT in (4), and can be added to  $k_0$  directly.

Let  $X_0$  be the input of activation layer in forward propagation, and  $\delta_Y$  be the error from the next layer. The error for the previous layer in backward propagation can be calculated by

$$\delta_X = \{1 - [\tanh(\Re(X_0))]^2\} \odot \Re(\delta_Y) + i\{1 - [\tanh(\Im(X_0))]^2\} \odot \Im(\delta_Y). \quad (10)$$

### 3.3 Pooling Layers

The pooling methods in SpecNet are implemented in the spatial domain after transforming the activated frequency feature maps back into the spatial domain using inverse FFT. As a result of the special convolution and activation function design to preserve conjugate symmetry structure of the feature maps in the spectral domain, the corresponding spatial feature maps are ensured to be real valued and the same pooling operation (max pooling or average pooling) used in standard CNNs can be used seamlessly in SpecNet. The calculation of the error in backward propagation can be found in the standard approach [34]. Note that the error is in the spatial domain, if the previous layer is either activation or convolutional layer, the error should be transformed into the spectral domain, i.e., to get  $\delta_Y$  in (3) or (10).

### 3.4 Implementation Details

In SpecNet, we store the kernels in spatial domain with size of  $N_k \times N_k$ . Therefore, given the input feature maps in spectral domain, each kernel should be upsampled to the same size of the inputs by adding zeros to the right and bottom of its value matrix, and then be transformed to spectral domain by using FFT. The complete forward propagation of the convolutional block (including convolution and activation operations) in spectral domain is shown in Algorithm 1.

## 4 Experiments

We demonstrate the feasibility of SpecNet using several benchmark datasets and by comparing the performance of SpecNet implementation of some state-of-the-art (LeNet, AlexNet, VGG16 and DenseNet) with their standard implementation.

### 4.1 Datasets

**MNIST** is a dataset of handwritten digits with 28 by 28 pixels each image, which is widely used for training and testing image processing, machine learning, and deep learning algorithms [1, 35]. In our experiment, 60,000 images were used for training and 10000 images were used for testing. The images were preprocessed by normalizing all pixel values to [0,1].

Table 1: Detailed network structure for DenseNet and SpecDenseNet

DenseNet			SpecDenseNet		
Layers	Output size	Structure	Layers	Output size	Structure
Input	$32 \times 32$	Input	Input	$32 \times 32$	Input
Convolution	$32 \times 32$	$3 \times 3$ kernel, BN, ReLU	Convolutional Block	$34 \times 34$	FFT
Pooling	$16 \times 16$	MaxPool (window size $2 \times 2$ )		$34 \times 34$	FConv2D ( $3 \times 3$ kernels), Activation
Dense Block	$16 \times 16$	$1 \times 1$ kernel, BN, ReLU		$32 \times 32$	IFFT
		$3 \times 3$ kernel, BN, ReLU $\times 6$	Pooling	$16 \times 16$	MaxPool (window size $2 \times 2$ )
Classification Layer	$1 \times 1$	GlobalAveragePool Fully-connected, SoftMax (10 classes)	Dense Block	$18 \times 18$	FFT
				$18 \times 18$	FConv2D ( $64 \times 3 \times 3$ kernels), Activation $\times 6$
				$16 \times 16$	FConv2D ( $64 \times 3 \times 3$ kernels), Activation $\times 6$
			Classification Layer	$1 \times 1$	IFFT
					GlobalAveragePool Fully-connected, SoftMax (10 classes)

**CIFAR-10** is a ten class dataset of small colored natural images [36]. In our experiment, 50,000 images were used for training and 10,000 images were used for testing. All images of CIFAR 10 were resized to 32 by 32 pixels, and each channel was normalized with respects to its mean and standard deviation [8]. Standard data augmentation techniques [7] were also applied to the training set.

**SVHN** is a dataset consisting of colored digit images with 32 by 32 pixels each image [37]. The dataset contains 99289 images: 73257 images for training and 26032 images for testing. It is reported that state-of-art CNNs can achieve good performance on the dataset without data augmentation [8], therefore we don't use any data augmentation for training. Besides, images were channel normalized by mean and standard deviation.

#### 4.2 Training

Training and evaluation of all networks were performed on a desktop computer running a 64-bit Linux operating system (Ubuntu 16.04) with an Intel Core i7-7700K CPU and 32 GB DDR4 RAM and two Nvidia GeForce GTX 1080 graphic cards (Nvidia driver 384.130) with 2560 CUDA cores and 8GB GDDR5 RAM. All networks and algorithms (including comparisons) were implemented in MATLAB 2018a and Tensorflow 1.09.

All the networks were trained by mini batch stochastic gradient descent (SGD) with a batch size of 64 on MNIST, CIFAR, and SVHN. The initial learning rate was set to 0.1 and was reduced by half every 50 epochs. The momentum of the optimizer was set to 0.95 and a total of 300 epochs was trained to ensure convergence.

#### 4.3 Results

First, we empirically show the impact when different thresholds are applied to the feature maps. The results are shown in Fig. 2. We apply two different thresholds ( $\beta = 0.5$  and  $\beta = 1.5$ ). Observe that the feature maps in the spectral domain are compressed (and sparsified), but that this does not significantly impact the feature maps in the spatial domain.

Next, we evaluated the proposed SpecNet using four widely used CNN architectures including LeNet-5 [29], AlexNet [38], VGG [39] and DenseNet [8] and we used prefix 'Spec' standing for the SpecNet implementation of each network. To ensure fair comparisons, the SpecNet implemented networks were made to have the same network hyper-parameters as their native spatial implementation. The experiments also remain the same conditions for image preprocessing, parameter initialization, and optimization settings. For example, architectures for DenseNet and SpecDenseNet were in Table 1. The other three networks were detailed in the supplementary material. The experimental results on MNIST, CIFAR-10 and SVHN are shown in Fig. 3.

Fig. 3 (a)(b)(c) compare the memory usage of the SpecNet implementation for the four different networks over a range of beta values from 0.5 to 1.5. We compute relative memory consumption and error by:  $\text{memory}(\text{error})$  of SpecNet / the  $\text{memory}(\text{error})$  in the original implementations. When compared with their original models, all SpecNet implementations of the four networks can save at least 50% memory with negligible loss of accuracy, indicating the feasibility of compressing feature maps within SpecNet framework. With increasing  $\beta$  value, all models show monotonic reduction of memory consumption. The rates of memory reduction are different between different network architectures, which is likely caused by different feature representation in various network design.

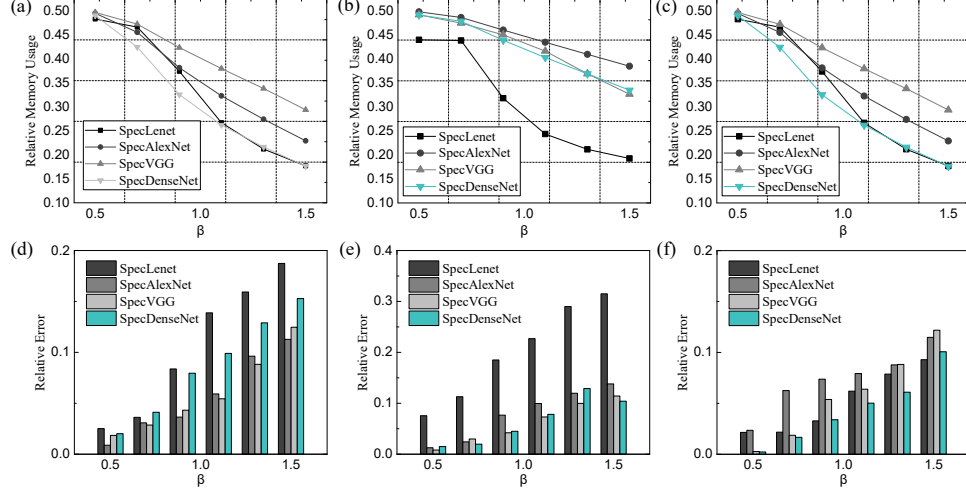


Figure 3: Memory consumption and testing performance of SpecNet compared with LeNet, AlexNet, VGG, and DenseNet [29, 38, 39, 8, 40] on three datasets. To make the comparison fair, we retain the analogous structures which we call SpecLeNet, SpecAlexNet, SpecVGG and SpecDenseNet. (a)(b)(c) relative memory consumption and (d)(e)(f) relative error of SpecNets tested on MNIST, CIFAR-10 and SVHN.

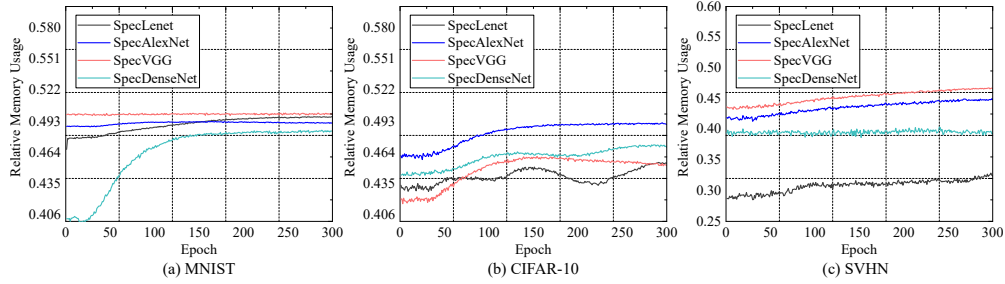


Figure 4: Memory consumption of SpecNet ( $\beta = 0.7$ ) during training compared with the original implementation of LeNet, AlexNet, VGG, and DenseNet on MNIST, CIFAR-10 and SHVN.

Figures 3 (d)(e)(f) compare the relative error of the SpecNet implementation for the four different networks over the same range of  $\beta$  values from 0.5 to 1.5. While the SpecNet typically compresses the models, there is penalty in the form of increased error in comparison to the original model with full spatial feature maps. The average accuracy of SpecAlexNet, SpecVGG, and SpecDenseNet can be higher than 95% when  $\beta$  is smaller than 1.0.

Figures 4 (a)(b)(c) shows the relative memory use ( $\beta = 0.7$ ) during the training process. We recorded average memory consumption of each epoch and compare it with memory in the original implementations. The memory consumption gradually improves with the training epochs, and the peak value tends to occur when the model has converged.

Table 2 shows a comparison between SpecNet and other recently published memory-efficient algorithms. The experiments were tested for memory usage when training VGG and DenseNet on the CIFAR-10 dataset. For each algorithm, we selected most memory efficient performance that still retains testing accuracy of at least 90%. The SpecNet outperformed all the listed algorithms and resulted in the lowest memory usage while maintaining high testing accuracy. It is notable that SpecNet is orthogonal to the work listed in the table, and these techniques can be applied to SpecNet to further reduce memory consumption.



Table 2: Comparison of relative memory usage for different memory efficient implementations applied to VGG and DenseNet. All the methods are tested on CIFAR-10.

	VGG	DenseNet
INPLACE-ABN [41]	0.52	0.58
Chen Meng et al. [42]	0.65	0.55
Memory-Efficient DenseNets [16]	N/A	0.44
vDNN [43]	0.38	0.39
<b>SpecNet</b>	<b>0.37</b>	<b>0.37</b>

## 5 Conclusion

We have introduced a new Convolutional Neural Network architecture called SpecNet, which performs both the convolution and the activation operations in the spectral domain. By setting a configurable threshold to force small values in the feature maps in the spectral domain to zero, the feature maps of SpecNet can be stored sparsely. SpecNet also employs a special activation function that preserves the sparsity of the feature maps and ensure training convergence. We have evaluated SpecNet on three competitive object recognition benchmark tasks (MNIST, CIFAR-10, and SVHN), and demonstrated the performance of SpecNet implementation of state-of-the-art (LeNet, AlexNet, VGG16 and DenseNet) to show the efficacy and efficiency for memory reduction. In some cases, SpecNet can reduce memory consumption by average 60% without significant loss of performance.

It is worth noting that our experimental hyper-parameter settings were for CNN in the spatial domain. Further memory reduction and performance improvement for SpecNet can be achieved by using more reasonable data scaling, dedicated network architecture and optimization settings tailored for SpecNet. The transform methods other than FFT such as DCT, Wavelet transform, can also be incorporated into SpecNet to promote energy concentration for memory reduction.

It is also notable that SpecNet is only focused on the sparse storage of feature maps in the spectral domain. In the future, we plan to apply aforementioned methods (such as model compression and scheduling) to SpecNet for more efficient use of memory.

## 6 Acknowledgement

We thank Prof. Varun Jog and Prof. Dimitris Papailiopoulos for helpful discussions.

## References

- [1] Yann LeCun, Yoshua Bengio, and Geoffrey Hinton. Deep learning. *nature*, 521(7553):436, 2015.
- [2] Yangyan Li, Rui Bu, Mingchao Sun, Wei Wu, Xinhan Di, and Baoquan Chen. Pointcnn: Convolution on x-transformed points. In *Advances in Neural Information Processing Systems*, pages 820–830, 2018.
- [3] Kristof Schütt, Pieter-Jan Kindermans, Huziel Enoc Saucedo Felix, Stefan Chmiela, Alexandre Tkatchenko, and Klaus-Robert Müller. Schnet: A continuous-filter convolutional neural network for modeling quantum interactions. In *Advances in Neural Information Processing Systems*, pages 991–1001, 2017.
- [4] Long Jin, Justin Lazarow, and Zhuowen Tu. Introspective classification with convolutional nets. In *Advances in Neural Information Processing Systems*, pages 823–833, 2017.
- [5] Fang Liu, Bochen Guan, Zhaoye Zhou, Alexey Samsonov, Humberto Rosas, Kevin Lian, Ruchi Sharma, Andrew Kanarek, John Kim, Ali Guermazi, et al. Fully automated diagnosis of anterior cruciate ligament tears on knee mr images by using deep learning. *Radiology: Artificial Intelligence*, 1(3):180091, 2019.
- [6] James Atwood and Don Towsley. Diffusion-convolutional neural networks. In *Advances in Neural Information Processing Systems*, pages 1993–2001, 2016.

- [7] Kaiming He, Xiangyu Zhang, Shaoqing Ren, and Jian Sun. Deep residual learning for image recognition. *CoRR*, abs/1512.03385, 2015.
- [8] Gao Huang, Zhuang Liu, Laurens Van Der Maaten, and Kilian Q Weinberger. Densely connected convolutional networks. In *Proceedings of the IEEE conference on computer vision and pattern recognition*, pages 4700–4708, 2017.
- [9] Yu Cheng, Duo Wang, Pan Zhou, and Tao Zhang. A survey of model compression and acceleration for deep neural networks. *CoRR*, abs/1710.09282, 2017.
- [10] Animesh Jain, Amar Phanishayee, Jason Mars, Lingjia Tang, and Gennady Pekhimenko. Gist: Efficient data encoding for deep neural network training. In *45th ACM/IEEE Annual International Symposium on Computer Architecture, ISCA 2018, Los Angeles, CA, USA, June 1-6, 2018*, pages 776–789, 2018.
- [11] Yunhe Wang, Chang Xu, Chao Xu, and Dacheng Tao. Beyond filters: Compact feature map for portable deep model. In *ICML*, volume 70 of *Proceedings of Machine Learning Research*, pages 3703–3711. PMLR, 2017.
- [12] Jiaxiang Wu, Cong Leng, Yuhang Wang, Qinghao Hu, and Jian Cheng. Quantized convolutional neural networks for mobile devices. *CoRR*, abs/1512.06473, 2015.
- [13] Matthieu Courbariaux and Yoshua Bengio. Binarynet: Training deep neural networks with weights and activations constrained to +1 or -1. *CoRR*, abs/1602.02830, 2016.
- [14] Stephen Jose Hanson and Lorian Y. Pratt. Comparing biases for minimal network construction with back-propagation. In D. S. Touretzky, editor, *Advances in Neural Information Processing Systems 1*, pages 177–185. Morgan-Kaufmann, 1989.
- [15] Emily Denton, Wojciech Zaremba, Joan Bruna, Yann LeCun, and Rob Fergus. Exploiting linear structure within convolutional networks for efficient evaluation. *CoRR*, abs/1404.0736, 2014.
- [16] Geoff Pleiss, Danlu Chen, Gao Huang, Tongcheng Li, Laurens van der Maaten, and Kilian Q Weinberger. Memory-efficient implementation of densenets. *arXiv preprint arXiv:1707.06990*, 2017.
- [17] Tianqi Chen, Bing Xu, Chiyuan Zhang, and Carlos Guestrin. Training deep nets with sublinear memory cost. *CoRR*, abs/1604.06174, 2016.
- [18] Junzhe Zhang, Sai-Ho Yeung, Yao Shu, Bingsheng He, and Wei Wang. Efficient memory management for gpu-based deep learning systems. *CoRR*, abs/1903.06631, 2019.
- [19] Suyog Gupta, Ankur Agrawal, Kailash Gopalakrishnan, and Pritish Narayanan. Deep learning with limited numerical precision. *CoRR*, abs/1502.02551, 2015.
- [20] R. Andri, L. Cavigelli, D. Rossi, and L. Benini. Yodann: An architecture for ultralow power binary-weight cnn acceleration. *IEEE Transactions on Computer-Aided Design of Integrated Circuits and Systems*, 37(1):48–60, Jan 2018.
- [21] Wei Wen, Chunpeng Wu, Yandan Wang, Yiran Chen, and Hai Li. Learning structured sparsity in deep neural networks. *CoRR*, abs/1608.03665, 2016.
- [22] Hao Li, Asim Kadav, Igor Durdanovic, Hanan Samet, and Hans Peter Graf. Pruning filters for efficient convnets. *CoRR*, abs/1608.08710, 2016.
- [23] Soravit Changpinyo, Mark Sandler, and Andrey Zhmoginov. The power of sparsity in convolutional neural networks. *CoRR*, abs/1702.06257, 2017.
- [24] Baoyuan Liu, Min Wang, Hassan Foroosh, Marshall Tappen, and Marianna Pensky. Sparse convolutional neural networks. In *Proceedings of the IEEE Conference on Computer Vision and Pattern Recognition*, pages 806–814, 2015.
- [25] Xiangyu Zhang, Jianhua Zou, Xiang Ming, Kaiming He, and Jian Sun. Efficient and accurate approximations of nonlinear convolutional networks. *CoRR*, abs/1411.4229, 2014.

- [26] Harry Pratt, Bryan M. Williams, Frans Coenen, and Yalin Zheng. Fcnn: Fourier convolutional neural networks. In *ECML/PKDD*, 2017.
- [27] Michaël Mathieu, Mikael Henaff, and Yann LeCun. Fast training of convolutional networks through ffts. In *ICLR*, 2014.
- [28] Shin Fujieda, Kohei Takayama, and Toshiya Hachisuka. Wavelet convolutional neural networks for texture classification. *CoRR*, abs/1707.07394, 2017.
- [29] Yann LeCun, LD Jackel, Leon Bottou, A Brunot, Corinna Cortes, JS Denker, Harris Drucker, I Guyon, UA Muller, Eduard Sackinger, et al. Comparison of learning algorithms for handwritten digit recognition. In *International conference on artificial neural networks*, volume 60, pages 53–60. Perth, Australia, 1995.
- [30] Alex Krizhevsky. One weird trick for parallelizing convolutional neural networks. *arXiv preprint arXiv:1404.5997*, 2014.
- [31] Christian Szegedy, Sergey Ioffe, Vincent Vanhoucke, and Alexander A Alemi. Inception-v4, inception-resnet and the impact of residual connections on learning. In *Thirty-First AAAI Conference on Artificial Intelligence*, 2017.
- [32] Jae-Han Lee, Minhyeok Heo, Kyung-Rae Kim, and Chang-Su Kim. Single-image depth estimation based on fourier domain analysis. In *Proceedings of the IEEE Conference on Computer Vision and Pattern Recognition*, pages 330–339, 2018.
- [33] Armin Kappeler, Sushobhan Ghosh, Jason Holloway, Oliver Cossairt, and Aggelos Katsaggelos. Ptychnet: Cnn based fourier ptychography. In *2017 IEEE International Conference on Image Processing (ICIP)*, pages 1712–1716. IEEE, 2017.
- [34] James Leonard and MA Kramer. Improvement of the backpropagation algorithm for training neural networks. *Computers & Chemical Engineering*, 14(3):337–341, 1990.
- [35] Li Deng. The mnist database of handwritten digit images for machine learning research [best of the web]. *IEEE Signal Processing Magazine*, 29(6):141–142, 2012.
- [36] Alex Krizhevsky and Geoffrey Hinton. Learning multiple layers of features from tiny images. Technical report, Citeseer, 2009.
- [37] Yuval Netzer, Tao Wang, Adam Coates, Alessandro Bissacco, Bo Wu, and Andrew Y Ng. Reading digits in natural images with unsupervised feature learning. 2011.
- [38] Alex Krizhevsky, Ilya Sutskever, and Geoffrey E Hinton. Imagenet classification with deep convolutional neural networks. In F. Pereira, C. J. C. Burges, L. Bottou, and K. Q. Weinberger, editors, *Advances in Neural Information Processing Systems 25*, pages 1097–1105. Curran Associates, Inc., 2012.
- [39] Karen Simonyan and Andrew Zisserman. Very deep convolutional networks for large-scale image recognition. *arXiv preprint arXiv:1409.1556*, 2014.
- [40] Yan Wang, Lingxi Xie, Chenxi Liu, Siyuan Qiao, Ya Zhang, Wenjun Zhang, Qi Tian, and Alan Yuille. Sort: Second-order response transform for visual recognition. In *Proceedings of the IEEE International Conference on Computer Vision*, pages 1359–1368, 2017.
- [41] Samuel Rota Bulò, Lorenzo Porzi, and Peter Kotschieder. In-place activated batchnorm for memory-optimized training of dnns. In *Proceedings of the IEEE Conference on Computer Vision and Pattern Recognition*, pages 5639–5647, 2018.
- [42] Chen Meng, Minmin Sun, Jun Yang, Minghui Qiu, and Yang Gu. Training deeper models by gpu memory optimization on tensorflow. In *Proc. of ML Systems Workshop in NIPS*, 2017.
- [43] Minsoo Rhu, Natalia Gimelshein, Jason Clemons, Arslan Zulfiqar, and Stephen W Keckler. vdn: Virtualized deep neural networks for scalable, memory-efficient neural network design. In *The 49th Annual IEEE/ACM International Symposium on Microarchitecture*, page 18. IEEE Press, 2016.

# Appendices

In experiment section, We compare SpecNet with four different commonly used CNN architectures: LeNet-5, AlexNet, VGG16 and DenseNet. In order to make a fair comparison, we use similar convolutional architectures as the four CNNs, we call them SpecLeNet, SpecAlexNet, SpecVGG, and SpecDenseNet. Detailed structures for DenseNet and SpecDenseNet are shown in Tab. 1, we report the rest three networks here:

Table 3: Detailed network structure for LeNet and SpecLeNet

LeNet			SpecLeNet		
Layers	Output size	Structure	Layers	Output size	Input
Input	28×28	Input	Input	28×28	Input
Convolution	24×24	Conv2D (6 5×5 kernels), ReLU	Convolutional Block	32×32	FFT
Pooling	12×12	MaxPool (window size 2×2)		32×32	FConv2D (6 5×5 kernels), Activation
Convolution	8×8	Conv2D (16 5×5 kernels), ReLU		24×24	IFFT
Pooling	4×4	MaxPool (window size 2×2)	Pooling	12×12	MaxPool (window size 2×2)
Classification Layer	1×10	FC(120 nodes) FC(80 nodes) SoftMax (10 classes)	Convolutional Block	15×15	FFT
				15×15	FConv2D (16 5×5 kernels), Activation
				8×8	IFFT
			Pooling	4×4	MaxPool (window size 2×2)
			Classification Layer	1×10	FC(120 nodes)
					FC(80 nodes)
					SoftMax (10 classes)

Table 4: Detailed network structure for AlexNet and SpecAlexNet

AlexNet			SpecAlexNet		
Layers	Output size	Structure	Layers	Output size	Structure
Input	32×32	Input	Input	32×32	Input
Convolution	32×32	Conv2D (24 3×3 kernels), ReLU	Convolutional Block	34×34	FFT
Pooling	16×16	MaxPool (window size 2×2)		34×34	FConv2D (24 3×3 kernels), Activation
Convolution	16×16	Conv2D (96 3×3 kernels), ReLU		32×32	IFFT
Pooling	8×8	MaxPool (window size 2×2)	Pooling	16×16	MaxPool (window size 2×2)
Convolution	8×8	Conv2D (192 3×3 kernels), BN, ReLU	Convolutional Block	18×18	FFT
		Conv2D (192 3×3 kernels), BN, ReLU		18×18	FConv2D (96 3×3 kernels), Activation
		Conv2D (96 3×3 kernels), BN, ReLU		16×16	IFFT
Pooling	4×4	MaxPool (window size 2×2)	Pooling	8×8	MaxPool (window size 2×2)
Classification	1×10	FC(1024 nodes) FC(1024 nodes) SoftMax (10 classes)	Convolutional Block	10×10	FFT
				10×10	FConv2D (192 3×3 kernels), Activation
				10×10	FConv2D (192 3×3 kernels), Activation
				10×10	FConv2D (96 3×3 kernels), Activation
				8×8	IFFT
			Pooling	4×4	MaxPool (window size 2×2)
			Classification	1×10	FC(1024 nodes)
					FC(1024 nodes)
					SoftMax (10 classes)

Table 5: Detailed network structure for VGG and SpecVGG

VGG-16			SpecVGG-16		
Layers	Output size	Structure	Layers	Output size	Structure
Input	32×32	Input	Input	32×32	Input
Convolution	32×32	Conv2D (64 3×3 kernels), BN, ReLU	Convolutional Block	34×34	FFT
		Conv2D (64 3×3 kernels), BN, ReLU		34×34	FConv2D (64 3×3 kernels), Activation
Pooling	16×16	MaxPool (window size 2×2)		34×34	FConv2D (64 3×3 kernels), Activation
Convolution	16×16	Conv2D (128 3×3 kernels), BN, ReLU		32×32	IFFT
		Conv2D (128 3×3 kernels), BN, ReLU	Pooling	16×16	MaxPool (window size 2×2)
Pooling	8×8	MaxPool (window size 2×2)	Convolutional Block	18×18	FFT
Convolution	8×8	Conv2D (256 3×3 kernels), BN, ReLU		18×18	FConv2D (128 3×3 kernels), Activation
		Conv2D (256 3×3 kernels), BN, ReLU		18×18	FConv2D (128 3×3 kernels), Activation
		Conv2D (256 3×3 kernels), BN, ReLU		16×16	IFFT
Pooling	4×4	MaxPool (window size 2×2)	Pooling	8×8	MaxPool (window size 2×2)
Classification	1×10	FC(512 nodes) SoftMax (10 classes)	Convolutional Block	10×10	FFT
				10×10	FConv2D (256 3×3 kernels), Activation
				10×10	FConv2D (256 3×3 kernels), Activation
				8×8	IFFT
			Pooling	4×4	MaxPool (window size 2×2)
				1×10	FC(512 nodes) SoftMax (10 classes)